Physics Letters B 797 (2019) 134797

Contents lists available at ScienceDirect

Physics Letters B

www.elsevier.com/locate/physletb

Evidence of octupole-phonons at high spin in ^{207}Pb

D. Ralet [a,b], E. Clément [b,*], G. Georgiev [a], A.E. Stuchbery [c], M. Rejmund [b], P. Van Isacker [b], G. de France [b], A. Lemasson [b], J. Ljungvall [a], C. Michelagnoli [b], A. Navin [b], D.L. Balabanski [d], L. Atanasova [u], A. Blazhev [g], G. Bocchi [e,ab], R. Carroll [f], J. Dudouet [h], E. Dupont [a], B. Fornal [i], S. Franchoo [aa], C. Fransen [g], C. Müller-Gatermann [g], A. Goasduff [k], A. Gadea [j], P.R. John [t,k], D. Kocheva [v], T. Konstantinopoulos [a], A. Korichi [a], A. Kusoglu [l], S.M. Lenzi [k], S. Leoni [e,ab], R. Lozeva [a,m], A. Maj [i], R. Perez [j], N. Pietralla [t], C. Shand [f], O. Stezowski [h], D. Wilmsen [b], D. Yordanov [aa], D. Barrientos [o], P. Bednarczyk [i], B. Birkenbach [g], A.J. Boston [p], H.C. Boston [p], I. Burrows [q], B. Cederwall [n], M. Ciemala [i], J. Collado [r], F. Crespi [e], D. Cullen [s], H.J. Eberth [g], J. Goupil [b], L. Harkness [p], H. Hess [g], A. Jungclaus [x], W. Korten [w], M. Labiche [q], R. Menegazzo [k], D. Mengoni [k], B. Million [e], J. Nyberg [y], Zs. Podolyák [f], A. Pullia [e], B. Quintana Arnés [z], F. Recchia [k], P. Reiter [g], F. Saillant [b], M.D. Salsac [w], E. Sanchis [r], C. Theisen [w], J.J. Valiente Dobon [o], O. Wieland [e]

[a] CSNSM, Univ. Paris-Sud, CNRS/IN2P3, Université Paris-Saclay, F-91405 Orsay, France
[b] GANIL, CEA/DRF-CNRS/IN2P3, Bd. Henri Becquerel, BP 55027, F-14076 Caen, France
[c] Department of Nuclear Physics, Australian National University, Canberra, ACT 2601, Australia
[d] ELI-NP, Horia Hulubei National Institute for R&D in Physics and Nuclear Engineering, 077125 Magurele, Romania
[e] Instituto Nazionale di Fisica Nucleare, Milano, I-20133 Milano, Italy
[f] Department of Physics, University of Surrey, Guildford, GU2 7XH, United Kingdom
[g] Institut für Kernphysik, Universität zu Köln, D-50937 Cologne, Germany
[h] Université de Lyon, Université Lyon-1, CNRS/IN2P3, UMR5822, IPNL, F-69622 Villeurbanne Cedex, France
[i] Institute of Nuclear Physics (IFJ), PAN, 31-342 Krakow, Poland
[j] Instituto de Física Corpuscular, CSIC-Universidad de Valencia, E-46071 Valencia, Spain
[k] Dipartimento di Fisica e Astronomia, Università degli Studi di Padova and INFN, Sezione di Padova, I-35131 Padova, Italy
[l] Department of Physics, Faculty of Science, Istanbul University, Vezneciler/Fatih, 34134, Istanbul, Turkey
[m] IPHC/CNRS-University of Strasbourg, F-67037 Strasbourg, France
[n] KTH Royal Institute of Technology, 10691 Stockholm, Sweden
[o] INFN, Laboratori Nazionali di Legnaro, Via Romea 4, I-35020 Legnaro, Italy
[p] Oliver Lodge Laboratory, The University of Liverpool, Oxford Street, Liverpool L69 7ZE, United Kingdom
[q] STFC Daresbury Laboratory, Daresbury, Warrington WA4 4AD, United Kingdom
[r] Department of Electronic Engineering, University of Valencia, E-46100 Burjassot (Valencia), Spain
[s] Schuster Building, School of Physics and Astronomy, The University of Manchester, Manchester M13 9PL, United Kingdom
[t] Institut für Kernphysik, Technische Universität Darmstadt, D-64289 Darmstadt, Germany
[u] Department of Medical Physics and Biophysics, Medical University-Sofia, 1431 Sofia, Bulgaria
[v] University of Sofia, Sofia, Bulgaria
[w] IRFU, CEA/DRF, Centre CEA de Saclay, F-91191 Gif-sur-Yvette Cedex, France
[x] Instituto de Estructura de la Materia, CSIC, E-28006 Madrid, Spain
[y] Department of Physics and Astronomy, Uppsala University, Uppsala, Sweden
[z] Laboratorio de Radiaciones Ionizantes, Universidad de Salamanca, E-37008 Salamanca, Spain
[aa] Institut de Physique Nucléaire, CNRS/IN2P3-Université Paris-Sud, F-91406 Orsay, France
[ab] Dipartimento di Fisica, Universita degli Studi di Milano, I-20133 Milano, Italy

ARTICLE INFO

Article history:
Received 2 July 2019
Accepted 19 July 2019
Available online 24 July 2019

ABSTRACT

A lifetime measurement of the $19/2^-$ state in ^{207}Pb has been performed using the Recoil Distance Doppler-Shift (RDDS) method. The nuclei of interest were produced in multi-nucleon transfer reactions induced by a ^{208}Pb beam impinging on a ^{100}Mo enriched target. The beam-like nuclei were detected

* Corresponding author.
E-mail address: clement@ganil.fr (E. Clément).

https://doi.org/10.1016/j.physletb.2019.134797

Editor: D.F. Geesaman

Keywords:
AGATA spectrometer
γ-Ray tracking
VAMOS++ spectrometer
Plunger device
Nuclear deformation
Octupole phonon

and identified in terms of their atomic mass number in the VAMOS++ spectrometer while the prompt γ rays were detected by the AGATA tracking array. The measured large reduced transition probability $B(E3, 19/2^- \rightarrow 13/2^+) = 40(8)$ W.u. is the first indication of the octupole phonon at high spin in ^{207}Pb. An analysis in terms of a particle-octupole-vibration coupling model indicates that the measured $B(E3)$ value in ^{207}Pb is compatible with the contributions from single-phonon and single particle $E3$ as well as $E3$ strength arising from the double-octupole-phonon 6^+ state, all adding coherently. A crucial aspect of the coupling model, namely the strong mixing between single-hole and the phonon-hole states, is confirmed in a realistic shell-model calculation.

The occurrence of collective vibrations, when a lattice of atoms or molecules oscillates uniformly at a single frequency forming a quantum-mechanical phonon, is a well-known phenomenon. Such vibrations correspond, in classical mechanics, to wave-like normal modes. Quantum-mechanical phonons, however, exhibit particle-like properties, too. The excitation spectra of several different many-body systems can be described as a superposition of elementary excitation modes that are (approximately independent) fluctuations about equilibrium. There is a close relation between the internal structure of the system and the nature of these fluctuations, which may lead to density vibrations or shape oscillations. In nuclei the character of collective vibrations follows from the observation that some are spherical, like doubly-magic nuclei, while others are deformed, like most rare-earth nuclei. In an intermediate situation the shape can undergo large fluctuations about one of the equilibrium shapes. In contrast to molecules, the nuclear energy scales related to vibrational and single-particle excitations are of the same order, and thus their interweaving has profound consequences.

Doubly-magic nuclei have a spherical equilibrium shape. Among them, the ^{208}Pb isotope, with $Z = 82$ protons and $N = 126$ neutrons, is the heaviest known doubly-magic nucleus. Its first-excited state has been established to be of natural-parity octupole type, $J^\pi = 3^-_c$, at an excitation energy of $E_x(3^-_c) = 2615$ keV, about 800 keV lower than the neutron shell-gap energy at $N = 126$, the index c stands for collective. The highly enhanced and collective transition connecting the 3^-_c level to the 0^+ ground state has been measured to have a reduced transition probability of $B(E3, 3^-_c \rightarrow 0^+) = 34.0(5)$ W.u. [1], that is, it exceeds by 34 times the Weisskopf unit or single-particle estimate. The 3^-_c state is interpreted as a one-phonon excitation corresponding to a nuclear surface vibration of octupole character while its microscopic structure is understood as the coherent and collective superposition of one-particle-one-hole (1p–1h) excitations across the neutron and proton shell gaps.

Provided that this 3^-_c state represents the first phonon of the octupole vibration, it is expected that the double-octupole quartet $(0^+_c, 2^+_c, 4^+_c, 6^+_c)$ of two-phonon states exists at an energy of about twice $E_x(3^-_c)$ [2]. In the case of a fully harmonic vibration, all members of this quartet, and in particular the 6^+_c level, decay to the one-phonon state with the characteristic reduced transition probability $B(E3, 6^+_c \rightarrow 3^-_c) = 2 \times B(E3, 3^-_c \rightarrow 0^+)$. Many attempts have been undertaken to identify the members of the two-phonon octupole quartet [3–11]. Candidates for the lower-spin members have been proposed [10,11] but the 6^+_c member has not been identified as yet. On the basis of a large-scale shell-model calculation, including up to 2p–2h excitations, Brown [12] concluded that the 6^+_c member of the double-octupole quartet is fragmented. Furthermore, he found that there are 0^+, 2^+, and 4^+ states with a concentrated double-octupole strength but decaying via weak $E1$ and $E2$ transitions, which in themselves are not strong evidence for the special double-octupole nature of a state.

In the nuclei neighboring ^{208}Pb, with one valence particle or hole, the particle-octupole-phonon model favors strong coupling between the orbitals $j_1 = l_1 \pm 1/2$ and $j_2 = l_2 \pm 1/2$ if $|j_1 - j_2| = |l_1 - l_2| = 3$, preserving the relative orientation of the spin and orbital angular momenta [13, (Vol. II, p. 419)]. In addition to the particle or hole states, several excitations have been found and interpreted as a collective octupole phonon $|3^-_c\rangle$ coupled to a particle or hole. Because of the strong coupling mentioned above, such states are expected to mix *i.e.* $|j_1^{(-1)}\rangle$ with $|j_2^{(-1)} \times 3^-_c; J_1 = j_1\rangle$ and $|j_1^{(-1)} \times 3^-_c; J_2\rangle$ with $|j_2^{(-1)} \times 6^+_c; J_2\rangle$, the latter being a particle or hole coupled to a double-octupole phonon. Given this mixing, it has been suggested in Ref. [14], in analogy to the case of ^{147}Gd [15], that the characteristic enhancement of the $B(E3, 6^+_c \rightarrow 3^-_c)$ value in ^{208}Pb, should be reflected in an enhanced $B(E3, J_2 \rightarrow J_1)$ value in the odd-mass nucleus.

The octupole excitations coupled to the low-spin ground state in ^{207}Pb have been investigated earlier [16,17]. The $5/2^+$ state at 2624 keV and $7/2^+$ state at 2662 keV have been interpreted as members of the low-spin $\nu p^{-1}_{1/2} \times \phi_1(3^-_c)$ multiplet resulting from weak coupling. The corresponding reduced transition probabilities have been measured as $B(E3, 5/2^+ \rightarrow 1/2-) = 30(3)$ W.u. and $B(E3, 7/2^+ \rightarrow 1/2-) = 28(2)$ W.u. [17]. The small positive energy shifts, +9 keV and +47 keV relative to $E_x(3^-_c)$, can be noticed that could be related to the blocking of the $\nu p_{1/2}$ orbital.

For ^{207}Pb, among the available neutron orbitals, $p_{1/2}$, $p_{3/2}$, $f_{5/2}$, $f_{7/2}$, $h_{9/2}$ and $i_{13/2}$, forming a major shell $82 \leq N \leq 126$, only the $j_1 = \nu i_{13/2}$ and $j_2 = \nu f_{7/2}$ satisfy the strong coupling rule, described above. The corresponding states, $13/2^+$ and $7/2^-$, dominantly of single-hole character, are well studied [18]. The $19/2^-$ state and the corresponding 2485 keV transition to the $13/2^+$ state were assigned to ^{207}Pb by Schramm et al. [6], and the $E3$ character of the transition was recently determined by Shand et al. [19]. The $13/2^+$, $7/2^-$, and $19/2^-$ states were analyzed in terms of particle-octupole-vibration coupling in Ref. [14] using the experimentally known level energies and assuming the dominance of the above-mentioned orbitals. This coupling scheme is depicted in Fig. 1. In panel (a) the one-phonon state is illustrated for ^{208}Pb. The coupled and uncoupled states in ^{207}Pb are shown in panels (b) and (c), respectively. The wave functions of the $13/2^+$ and $19/2^-$ states are represented as single-hole states and single-hole states coupled to a single or double octupole phonon in ^{208}Pb. The coefficients α_i and β_i, as shown in panel (d) of Fig. 1, depend crucially on the mixing matrix element $h \equiv \langle \nu i^{-1}_{13/2} | \hat{V} | \nu f^{-1}_{7/2} \times 3^-_c; 13/2^+\rangle$, which can be calculated in a variety of ways. Its absolute value can be deduced from the excitation energies of the $13/2^+$, $7/2^-$, and $19/2^-$ levels in ^{207}Pb, leading to $|h| = 0.725$ MeV [14]. Alternatively, it is obtained in the context of the particle-vibration coupling model [13, (Vol. II, p. 418)], where it depends on the radial overlap of the particles and the oscillating potential at the surface of the nucleus and the zero point amplitude of the nuclear vibration. Hamamoto [20] for the case of ^{207}Pb obtained the value

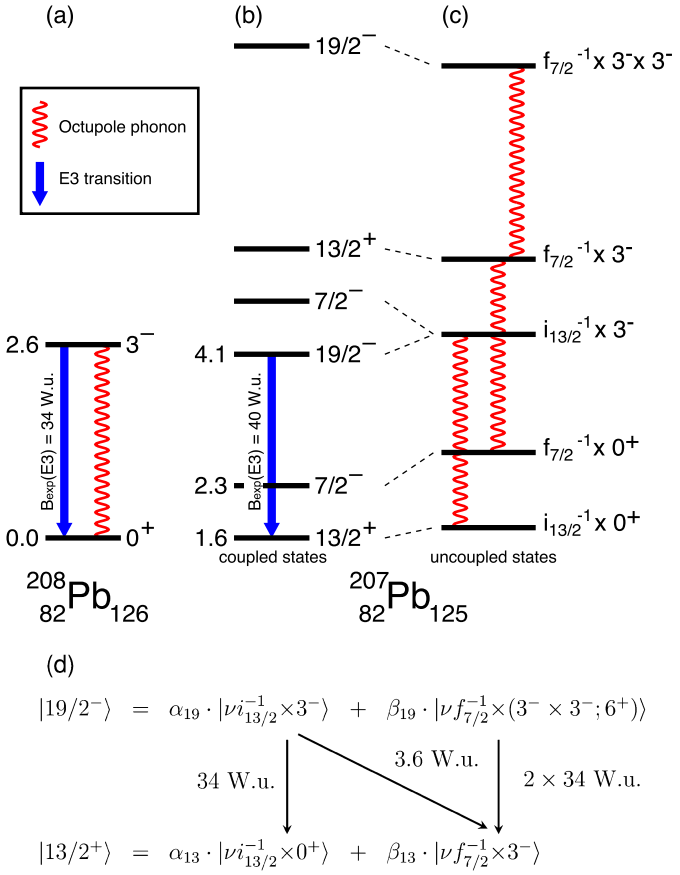

Fig. 1. Illustration of the particle-octupole-vibration coupling model: (a) The lowest octupole-vibrational phonon of ^{208}Pb, (b) selected states resulting from the particle-octupole-vibration coupling in ^{207}Pb, (c) uncoupled (unperturbed) states in ^{207}Pb, (d) wave functions of the $13/2^+$ and $19/2^-$ states in the particle-octupole-vibration coupling model. The energies of the known states are given in MeV.

of $h = 0.710$ MeV. Finally, it can also be calculated with the shell-model expression, where the particle-hole matrix elements can be obtained from particle-particle matrix elements using the Pandya transformation [21]

$$h = \sqrt{\frac{1}{2}}\left(\sum_{kk'} a^{\nu}_{kk'}\langle \nu f_{7/2}\nu i^{-1}_{13/2}; 3^-|\hat{V}_{\nu\nu}|j_{\nu k}j^{-1}_{\nu k'}; 3^-\rangle + \sum_{ll'} a^{\pi}_{ll'}\langle \nu f_{7/2}\nu i^{-1}_{13/2}; 3^-|\hat{V}_{\nu\pi}|j_{\pi l}j^{-1}_{\pi l'}; 3^-\rangle\right),$$

which gives the separate contributions of the neutron-neutron ($\nu\nu$) and neutron-proton ($\nu\pi$) interactions. The sums are over the neutron and proton particle-hole excitations that constitute the octupole phonon. The amplitudes $a^{\nu}_{kk'}$ and $a^{\pi}_{ll'}$ are obtained microscopically in a shell-model calculation for ^{208}Pb with 24 single-particle energies taken from Ref. [22] and with the realistic nucleon-nucleon interaction as given in Ref. [23]. Although the off-diagonal matrix elements in the expression for h generally are small and of varying sign, multiplied with amplitudes they act coherently, giving rise to a large mixing matrix element with the value of $h = 0.655$ MeV. This is the hallmark of collective behavior, which therefore is found to be present in a realistic shell-model description. The consistency of the values for the mixing matrix element derived with three totally different approaches lends support to the hole-octupole-phonon interpretation of states in ^{207}Pb. In the following the experimental value of $h = 0.725$ MeV is used.

The experimental value of $h = 0.725$ MeV was determined assuming the contribution of the collective vibrational-phonons to the $13/2^+$ and $19/2^-$ states. Due to the presence of the specific orbits, the $f_{7/2}$ and $i_{13/2}$ for ^{207}Pb, a strong particle-octupole-vibration coupling is expected to attract an admixture of the double octupole state to the low-lying yrast $19/2^-$ state, that can decay by the characteristic enhanced $E3$ transition. The main part of the double octupole state remains however in the higher lying $19/2^-$, which could be fragmented and have different decay modes. The negative energy shift of -130 keV for the 2485 keV transition between the $19/2^-$ and $13/2^+$, relative to $E_x(3^-_c)$, is therefore understood as resulting from the mixing of one-phonon state with the two-phonon state. The large $B(E3, 19/2^- \rightarrow 13/2^+)$ value, characterizing the contribution of octupole phonons, has however not been measured. A predicted $B(E3, 19/2^- \rightarrow 13/2^+)$ value is obtained (see discussion below) that is enhanced as compared to $B(E3, 3^-_c \rightarrow 0^+)$ in ^{208}Pb, due to the strong mixing and the coherent contribution of the single-phonon and single particle and the double-octupole-phonon strengths. The aim of this work was to provide the experimental evidence of the collective nature of the $E3$ $(19/2^- \rightarrow 13/2^+)$ transition by means of lifetime measurement. The knowledge of the strength of this transition will allow to prove the hypothesis of the strong coupling scheme and quantify the contributions of one-phonon and two-phonon states; ultimately it may prove the existence of the latter.

The measurement of sub-nanosecond lifetimes of high spin states in nuclei near ^{208}Pb is very challenging. These high spin states can be efficiently populated in multi-nucleon transfer reactions of heavy ions at the energies near the Coulomb barrier [6,14,23]. The excited products of interest are distributed near the grazing angle, far away from the beam axis, in contrast to fusion reactions. Multi-nucleon transfer reactions produce hundreds of nuclei at the same time, therefore some selection of the reaction products is required. It can be obtained using $\gamma - \gamma$ coincidences or using a mass analyzer or magnetic spectrometer to determine the mass number. The direct measurement of the atomic number at $Z \sim 82$ for low energy ions is not possible today. Mass analyzers have typically low acceptance and are restricted to operation near 0°. Further, the use of the plunger technique, for measurement of sub-nanosecond lifetimes of states populated in multi-nucleon transfer reactions, requires an event-by-event measurement of the recoil velocity vector. In this work the VAMOS++ spectrometer was used to identify, for the first time, the atomic mass number of the lead-like ejectiles at energies ranging from 1 to 2 MeV/u. The required mass resolution was reached only for a part of the focal plane setup ($\sim$ 15%), which resulted in reduced statistics. In this letter we present the results of the first lifetime measurement of the $J^\pi = 19/2^-$ level in ^{207}Pb, proving the one-octupole phonon nature of this state and suggesting the existence of a double-octupole 6^+_c state in ^{208}Pb.

The experiment was performed at the Grand Accélérateur National d'Ions Lourds, Caen, France using the RDDS method [24], in combination with a multi-nucleon transfer reaction in inverse kinematics. A ^{208}Pb beam at 6.25A MeV impinged on an enriched 1.9 mg/cm^2-thick ^{100}Mo target followed by a 2 mg/cm^2-thick Ni degrader. Beam-like reaction products were detected and identified on an event-by-event basis in the large-acceptance VAMOS++ spectrometer [25,26]. The optical axis of the spectrometer was positioned at 26° with respect to the beam axis, at the grazing angle of the beam-like products. The VAMOS++ spectrometer allowed the identification of the reaction products in mass-over-charge (A/Q) and atomic charge (Q), and provided the velocity vector ($\vec{V}$) necessary for the Doppler correction.

Fig. 2 shows a typical two-dimensional identification matrix obtained in the present experiment. The X-axis represents the mass-

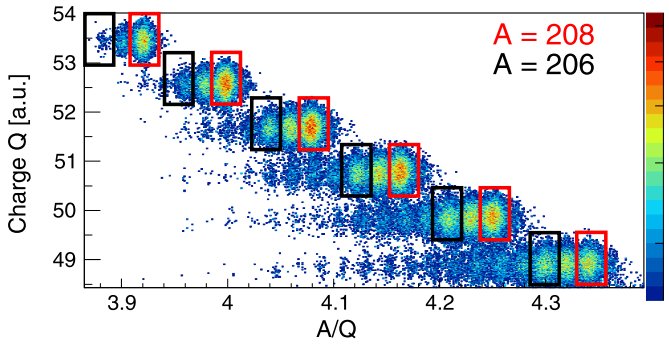

Fig. 2. Two-dimensional identification matrix obtained with the VAMOS++ spectrometer. Nuclei with atomic mass number $A = 206$ and $A = 208$ are highlighted for several charge states measured in the spectrometer. Due to the low velocity of the recoils, an element identification (Z) is not possible.

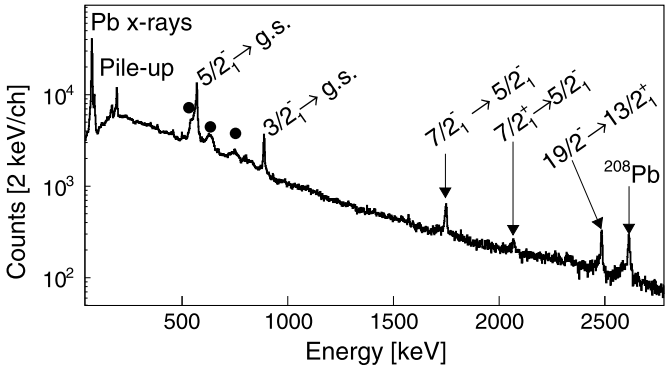

Fig. 3. γ-Ray spectrum gated on mass $A = 207$ at the target-to-degrader distance of 75 µm. The transitions marked with a circle correspond to the Coulomb excitation of the ^{100}Mo target, Doppler corrected using the velocity vector of the heavy partner.

over-charge ratio as a function of the atomic-charge state. Mass resolution of $\sim 0.9/208$ (FWHM) was obtained. The analysis procedure is further detailed in Ref. [27]. Excited-state half-lifes ($T_{1/2}$) were measured using the RDDS technique with the plunger device of the University of Cologne [28]. Doppler-corrected prompt γ rays, emitted before and after the Ni degrader foil, were measured by the HPGe AGATA tracking array [29,30] placed at backward angles in a compact geometry (target-to-detector distance of 148.5 mm). The γ-ray energy Doppler correction was performed using the recoil velocity ($\vec{V}$), obtained from the VAMOS++ spectrometer, after the Ni degrader, and the position of the first γ-ray interaction obtained from the Orsay Forward Tracking algorithms using standard parameters [31].

Fig. 3 shows the Doppler-corrected γ-ray spectrum measured in the AGATA spectrometer, selected with mass $A = 207$ in the VAMOS++ spectrometer for the 75 µm target-to-degrader distance. Transitions at 570 keV, 898 keV, 1770 keV, and 2485 keV belong to ^{207}Pb. The 2067 keV line corresponds to the shifted component of the short-lived ($T_{1/2} = 660$ fs [32]) $7/2^+_1$ state decay in ^{207}Pb to the $5/2^-_1$ state. The transition at 2615 keV corresponds to the 3^-_c state decay in ^{208}Pb; it is a contaminant from the random coincidence resulting from the inelastic scattering of the beam. The transitions marked with a circle correspond to the ^{100}Mo decay following Coulomb excitation, Doppler corrected using the velocity vector of the beam-like ion, measured after the degrader.

Fig. 4 shows Doppler corrected γ-ray spectra measured in the AGATA spectrometer, selected on mass $A = 207$ in the VAMOS++ spectrometer, for five target-to-degrader distances (75 µm, 200 µm, 625 µm, 1000 µm, and 2000 µm) for the relevant transitions used for the lifetime measurement. Since the Doppler correction used the velocity measured after the degrader, the unshifted (U) component corresponds to the events where the γ-ray was emitted after the degrader and shifted (S) to the events where gamma-ray was emitted before the degrader. The velocity of ions detected in VAMOS++ ranged from 14 to 22 µm/ps, and the decrease of the velocity in the degrader was typically about 13%. Events with a relative angle greater than 138°, between the γ-ray and the outgoing-particle velocity vector, were selected to enhance the clear separation between the shifted (S) and unshifted (U) components of the γ-ray transitions. The parameters required for the Doppler correction using the AGATA and VAMOS++ spectrometers were obtained using the inelastic scattering of the ^{208}Pb in a data set without the thick Ni degrader. On the left panel of Fig. 4, the two components, shifted (S) at 2454 keV and unshifted (U) at 2485 keV, of the $19/2^- \rightarrow 13/2^+$ transition in ^{207}Pb are observed.

Within the RDDS technique, a decay curve was constructed from the intensities of the unshifted ($U_{19/2^-}$) component of the $19/2^- \rightarrow 13/2^+$ transition normalized to the $7/2^-_1 \rightarrow 5/2^-_1$ transition in ^{207}Pb as a function of the target-to-degrader distance. The $7/2^-_1$ state, at an excitation energy of 2339.9 keV, decays by a γ-ray transition of 1770.2 keV to the first-excited $5/2^-_1$ state. Only the shifted component ($S_{7/2^-}$) was observed due to the very short lifetime of the $7/2^-_1$ state (see right panel of Fig. 4). The γ-ray transition intensities were determined assuming for all distances the same width and centroid for the peaks. The normalization using the sum of the shifted ($S_{19/2^-}$) and unshifted ($U_{19/2^-}$) components of the 2485 keV transition is in agreement, within the statistical uncertainties, with the normalization using the $7/2^-_1 \rightarrow 5/2^-_1$ transition. The former has a higher statistical error due to the weak intensity of the shifted ($S_{19/2^-}$) component. In the following, all quoted errors are statistical. In agreement with the level scheme of ^{207}Pb [19], γ-γ-coincidence analysis showed two transitions above the $13/2^+$ state populating the $19/2^-$ state: the $21/2^- \rightarrow 19/2^-$ and $23/2^- \rightarrow 19/2^-$ transitions with the respective energies of 592 keV and 749 keV and feeding of 20(6)% and 37(5)%, respectively. These states, having a very long effective lifetime, are taken into account in the analysis, following the method described in Ref. [24]. The lifetime was extracted from the first three distances where the RDDS analysis showed maximum sensitivity. The lifetime analysis procedure was verified using the known decay of the 2^+_1 state in ^{206}Pb ($T_{1/2} = 8.30(24)$ ps [33]). The deduced value from this experiment is $T_{1/2} = 12(3)$ ps, taking into account the feedings from the 3^+ and 4^+ states, in reasonable agreement with the published value.

The result of the lifetime analysis for the $19/2^-$ state decaying by the 2485 keV transition in ^{207}Pb is presented in Fig. 5. The deduced value of $T_{1/2} = 20(4)$ ps, corresponds to $B(E3, 19/2^- \rightarrow 13/2^+) = 40(8)$ W.u., assuming a branching ratio of 100%. When compared with the $B(E3, 3^-_c \rightarrow 0^+) = 34.0(5)$ W.u. in ^{208}Pb, it is a clear first indication that the octupole-vibrations play an important role in the nature of the $19/2^-$ state. Further, the different contributions to the octupole strength can be evaluated. With the wave functions of the $19/2^-$ and $13/2^+$ states as given in Fig. 1(d) and with the two-to-one-phonon strength $B(E3, 6^+_c \rightarrow 3^-_c) = 2 \times B(E3, 3^-_c \rightarrow 0^+)$, the reduced transition matrix element can be written as follows:

$$\langle 13/2^+ || E3 || 19/2^- \rangle = \sqrt{\frac{20}{7}} \cdot \langle 0^+ || E3 || 3^-_c \rangle \cdot (\alpha_{19} \cdot \alpha_{13} + \sqrt{2} \cdot \beta_{19} \cdot \beta_{13}) + \sqrt{\frac{10}{7}} \cdot \langle \nu f^{-1}_{7/2} || E3 || \nu i^{-1}_{13/2} \rangle \cdot \alpha_{19} \cdot \beta_{13}$$

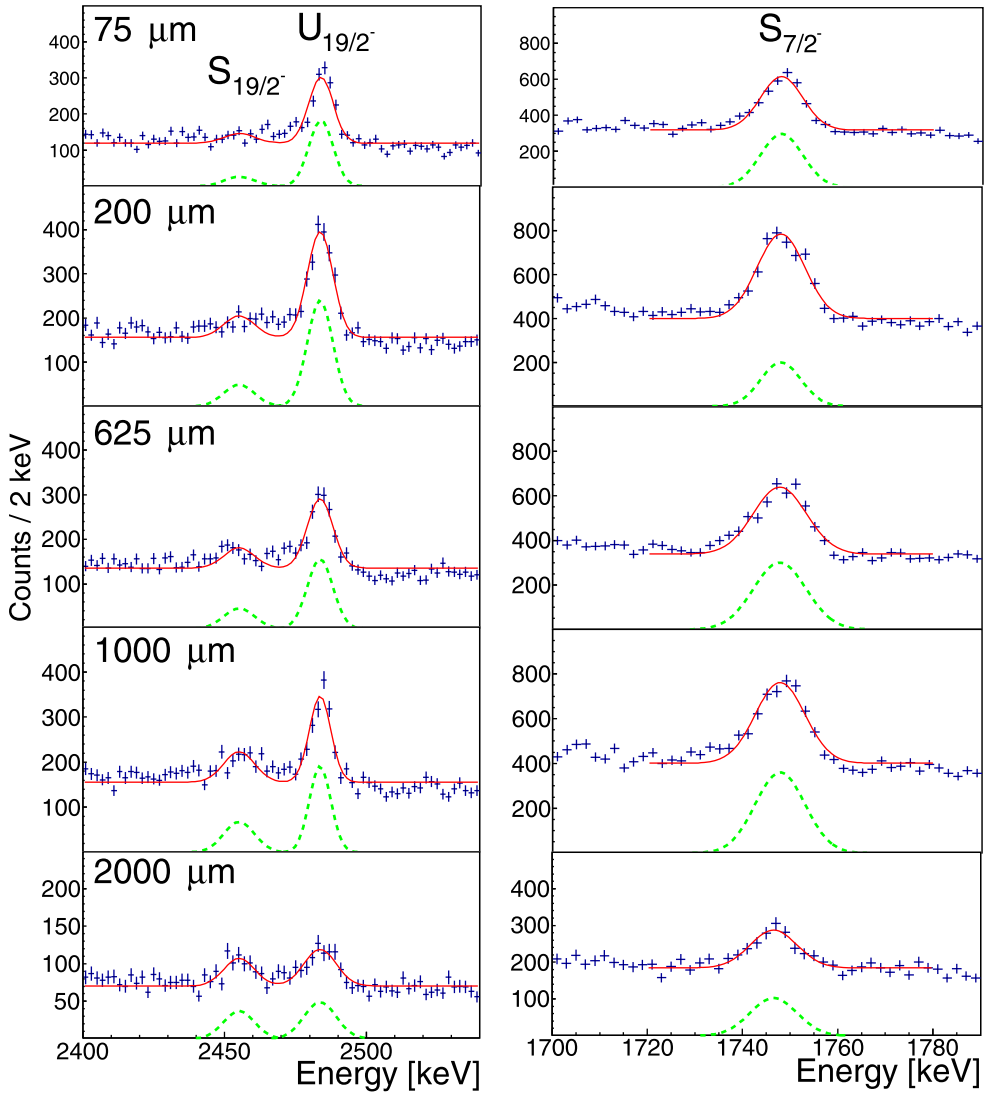

Fig. 4. Doppler corrected γ-ray spectra for mass $A = 207$ as a function of the target-to-degrader distance. Left: the $19/2^- \rightarrow 13/2^+$ transition in ^{207}Pb. Right: the $7/2^-_1 \rightarrow 5/2^-_1$ transition in ^{207}Pb used for normalization.

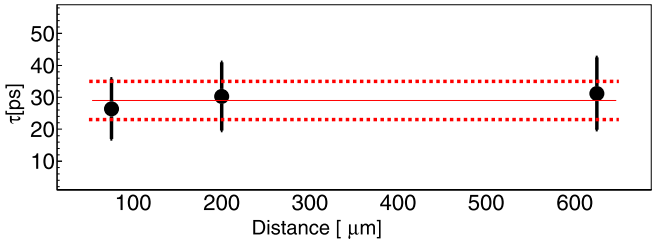

Fig. 5. Mean lifetime (τ) determination of the $19/2^-$ state of ^{207}Pb. The continuous red line corresponds to the fitted mean value of τ as the dashed lines correspond to its 1σ error bar.

The coefficients α and β can be taken from the analysis in [14]. With Woods-Saxon radial wave functions and an effective charge $e_{\text{eff}} = 1.35(45)e$, one obtains the single-hole reduced matrix element $\langle \nu f^{-1}_{7/2} \| E3 \| \nu i^{-1}_{13/2} \rangle = -359(119)\ e\ \text{fm}^3$ [14]. The errors associated with the effective charge and the reduced transition matrix element follow from the experimental precision of the $B(E3, 15/2^- \rightarrow 9/2^+)$ in ^{209}Pb [34]. The first term in the equation, proportional to $\alpha_{19}\alpha_{13}$ multiplied with the collective $E3$ matrix element, provides the dominant contribution, with corrections stemming from the two-to-one-phonon $6^+_c \rightarrow 3^-_c$ transition (second term, proportional to $\beta_{19}\beta_{13}$) and the single-hole $\nu i^{-1}_{13/2} \rightarrow \nu f^{-1}_{7/2}$ transition (third term, proportional to $\alpha_{19}\beta_{13}$).

Three different scenarios can be considered along with the calculated reduced transition probability (in parentheses): (i) Neglecting the strong coupling and the two-phonon contribution using $\alpha_{19} = \alpha_{13} = 1$ and $\beta_{19} = \beta_{13} = 0$ (34.0(5) W.u.) (ii) Neglecting the two-phonon contribution using $\alpha_{19} = 1$, $\alpha_{13} = 0.98$, $\beta_{19} = 0$ and $\beta_{13} = -0.19$ (37(2) W.u.) (iii) Considering all the contributions using $\alpha_{19} = 0.97$, $\alpha_{13} = 0.98$, $\beta_{19} = -0.25$ and $\beta_{13} = -0.19$ (40(2) W.u.). The errors associated with the calculated values result from those of $B(E3, 3^-_c \rightarrow 0^+)$ in ^{208}Pb and e_{eff}. The observed strength and a comparison with the above calculated values suggest an enhancement with respect to the known $B(E3, 3^-_c \rightarrow 0^+)$ in ^{208}Pb. All contributions, including the two-phonon state, add coherently to reach maximum collectivity. The measured value is compatible, within the error bar, with the predicted value. However the experimental uncertainty remains too large to disentangle the presence of the strong particle-octupole coupling and the two-phonon state. To achieve this goal, the experimental uncertainty for the case of ^{207}Pb has to reach at least the level of 2%. Further, a more precise determination of the effective charge, which

is a main source of uncertainties in the calculations, would be required.

In summary, a large $B(E3, 19/2^- \rightarrow 13/2^+) = 40(8)$ W.u. reduced transition probability has been measured in ^{207}Pb based on the lifetime measurement of the $19/2^-$ state using the RDDS technique. Such collective character indicates that the dominant component of this state is a single-hole excitation coupled to the octupole phonon of the ^{208}Pb core. The energy lowering of the 2485 keV transition in ^{207}Pb, as compared to the 2615 keV transition in ^{208}Pb, is consistent with a mixing with a state containing the double-octupole-phonon excitation. The measured reduced transition probability is compatible with a contribution from the two-to-one-octupole-phonon $E3$ transition. Further information on the double-octupole-phonon state can be obtained by a more precise lifetime measurement of the $19/2^-$ state in ^{207}Pb or of the corresponding $21/2^+$ state in ^{209}Pb, where the $B(E3)$ was predicted to be 50 W.u. [14]. In addition, a more accurate measurement of the lifetime of the $15/2^-$ state in ^{209}Pb is mandatory to improve the precision of the $E3$ effective charge.

The authors are grateful for the help of the GANIL staff and of the AGATA collaboration. D. R. Chakrabarty is gratefully acknowledged for the careful reading of the manuscript. This work was supported by the European Union Seventh Framework through ENSAR (Contract No. 262010) and partly funded by the P2IO LabEx (ANR-10-LABX-0038) in the framework Investissements dávenir (ANR-11-IDEX-0003-01) managed by the French National Research Agency (ANR). DLB is supported by the Extreme Light Infrastructure Nuclear Physics (ELI-NP) Phase II, a project co-financed by the Romanian Government and the European Union through the European Regional Development Fund - the Competitiveness Operational Programme (1/07.07.2016, COP, ID 1334). This work was supported by the Bundesministerium für Bildung und Forschung under grant No. 05P18RDFN9. A.G and R.P were partially supported by Ministry of Science, Spain, under the Grants FPA2017-84756-C4 and SEV-2014-0398, and by the EU FEDER funds. A.E.S was partially supported by the Australian Research Council grant No. DP0773273. This work was supported by the National Science Center (NCN), Poland under HARMONIA contract No. 2016/22/M/ST2/00269.

References

[1] R.H. Spear, et al., Phys. Lett. B 128 (1) (1983) 29–32, https://doi.org/10.1016/0370-2693(83)90067-9.
[2] J. Blomqvist, Phys. Lett. B 33 (8) (1970) 541–544, https://doi.org/10.1016/0370-2693(70)90342-4.
[3] M.A.J. Mariscotti, et al., Nucl. Phys. A 407 (1) (1983) 98–126, https://doi.org/10.1016/0375-9474(83)90310-X.
[4] R. Julin, et al., Phys. Rev. C 36 (1987) 1129–1131, https://doi.org/10.1103/PhysRevC.36.1129.
[5] H.J. Wollersheim, et al., Z. Phys. A 341 (2) (1992) 137–144, https://doi.org/10.1007/BF01298473.
[6] M. Schramm, et al., Z. Phys. A 344 (1) (1992) 121–122, https://doi.org/10.1007/BF01291029.
[7] B.D. Valnion, et al., Z. Phys. A 350 (1) (1994) 11–12, https://doi.org/10.1007/BF01285046.
[8] C. Fahlander, et al., Phys. Scr. 1995 (T56) (1995) 243.
[9] E.F. Moore, et al., Nucl. Instrum. Methods Phys. Res., Sect. B, Beam Interact. Mater. Atoms 99 (1) (1995) 308–311, https://doi.org/10.1016/0168-583X(94)00687-3.
[10] M. Yeh, et al., Phys. Rev. Lett. 76 (8) (1996) 1208–1211, https://doi.org/10.1103/PhysRevLett.76.1208.
[11] M. Yeh, et al., Phys. Rev. C 57 (5) (1998) R2085–R2089, https://doi.org/10.1103/PhysRevC.57.R2085.
[12] B.A. Brown, Phys. Rev. Lett. 85 (25) (2000) 5300–5303, https://doi.org/10.1103/PhysRevLett.85.5300.
[13] A. Bohr, B.R. Mottelson, Nuclear Structure, World Scientific, 1998.
[14] M. Rejmund, et al., Eur. Phys. J. A 8 (2) (2000) 161–164, https://doi.org/10.1007/s100500070102.
[15] P. Kleinheinz, et al., Phys. Rev. Lett. 48 (1982) 1457–1461, https://doi.org/10.1103/PhysRevLett.48.1457.
[16] E. Grosse, et al., Nucl. Phys. A 174 (3) (1971) 525–538, https://doi.org/10.1016/0375-9474(71)90400-3.
[17] O. Häusser, et al., Nucl. Phys. A 194 (1) (1972) 113–139, https://doi.org/10.1016/0375-9474(72)91055-X.
[18] F.G. Kondev, S. Lalkovski, Nucl. Data Sheets 112 (3) (2011) 707–853, https://doi.org/10.1016/j.nds.2011.02.002.
[19] C. Shand, et al., Acta Phys. Pol. B 46 (3) (2015) 619, https://doi.org/10.5506/APhysPolB.46.619.
[20] I. Hamamoto, Phys. Rep. 10 (2) (1974) 63–105, https://doi.org/10.1016/0370-1573(74)90019-2.
[21] S.P. Pandya, Phys. Rev. 103 (4) (1956) 956–957, https://doi.org/10.1103/PhysRev.103.956.
[22] M. Rejmund, et al., Phys. Rev. C 59 (5) (1999) 2520–2536, https://doi.org/10.1103/PhysRevC.59.2520.
[23] J. Wrzesiński, et al., Eur. Phys. J. A 10 (3) (2001) 259–265, https://doi.org/10.1007/s100500170111.
[24] A. Dewald, et al., Z. Phys. A 334 (2) (1989) 163–175, https://doi.org/10.1007/BF01294217.
[25] M. Rejmund, et al., Nucl. Instrum. Methods Phys. Res., Sect. A, Accel. Spectrom. Detect. Assoc. Equip. 646 (1) (2011) 184–191, https://doi.org/10.1016/j.nima.2011.05.007.
[26] M. Vandebrouck, et al., Nucl. Instrum. Methods Phys. Res., Sect. A, Accel. Spectrom. Detect. Assoc. Equip. 812 (2016) 112–117, https://doi.org/10.1016/j.nima.2015.12.040.
[27] D. Ralet, et al., Phys. Scr. 92 (5) (2017) 054004.
[28] A. Dewald, et al., Prog. Part. Nucl. Phys. 67 (3) (2012) 786–839, https://doi.org/10.1016/j.ppnp.2012.03.003.
[29] S. Akkoyun, et al., Nucl. Instrum. Methods Phys. Res., Sect. A, Accel. Spectrom. Detect. Assoc. Equip. 668 (2012) 26–58, https://doi.org/10.1016/j.nima.2011.11.081.
[30] E. Clément, et al., Nucl. Instrum. Methods Phys. Res., Sect. A, Accel. Spectrom. Detect. Assoc. Equip. 855 (2017) 1–12, https://doi.org/10.1016/j.nima.2017.02.063.
[31] A. Lopez-Martens, et al., Nucl. Instrum. Methods Phys. Res., Sect. A, Accel. Spectrom. Detect. Assoc. Equip. 533 (3) (2004) 454–466, https://doi.org/10.1016/j.nima.2004.06.154.
[32] O. Häusser, et al., Nucl. Phys. A 194 (1) (1972) 113–139, https://doi.org/10.1016/0375-9474(72)91055-X.
[33] F. Kondev, Nucl. Data Sheets 109 (6) (2008) 1527–1654, https://doi.org/10.1016/j.nds.2008.05.002.
[34] C. Ellegaard, et al., Phys. Lett. B 25 (8) (1967) 512–514, https://doi.org/10.1016/0370-2693(67)90224-9.